ISSN 0027-1314, Moscow University Chemistry Bulletin, 2007, Vol. 62, No. 3, pp. 119–122. © Allerton Press, Inc., 2007.
Original Russian Text © I.S. Tkachenko, V.I. Gibalov, V.V. Lunin, 2007, published in Vestnik Moskovskogo Universiteta. Khimiya, 2007, No. 3, pp. 147–151.

Breakdown of a Gas Gap in a Surface Barrier Discharge

I. S. Tkachenko, V. I. Gibalov, and V. V. Lunin

Department of Physical Chemistry
e-mail: tcorporation@narod.ru

Received June 12, 2006

Abstract—The processes that occur in a surface barrier discharge in oxygen at atmospheric pressure have been studied by numerical modeling. Modeling is performed assuming the existence of local equilibrium, and the dynamics of charged particles in the gas gap is calculated using continuity equations. The configuration of the electric field in the discharge zone is determined by integration of the Poisson equation. It turns out that the breakdown of the gas gap is determined by the photoemission from the cathode surface. The appearance and development of the microdischarge channel are sustained by the cathode layer that is formed at the conducting cathode. The parameters of the cathode layer obtained in oxygen at atmospheric pressure are virtually the same as for the ordinary cathode layer of the glow discharge.

DOI: 10.3103/S0027131407030017

A barrier discharge of any configuration is a unique plasmachemical reactor that makes it possible to carry out relatively simply nonequilibrium chemical synthesis, including the synthesis of ozone, on an industrial scale [1]. The dynamics of processes in coplanar and volume barrier discharges has been extensively studied [2–4]. So-called creeping discharges have been little studied. Studies of fast processes above the dielectric surface [5–7] left some unresolved questions. The present work deals with the systematic and detailed study of the dynamics of processes in a surface barrier discharge, including the kinetics of ozone synthesis.

FORMULATION OF THE PROBLEM

A barrier discharge is developed on the surface of the dielectric of a discharge cell when a high voltage is applied to high-voltage electrodes (Fig. 1). High-voltage electrodes can be of different shape, and any number of them can be in the system. The discharge in such a system is developed normally to the electrode surface along the dielectric surface in the form of thin discharge channels, microdischarges (Fig. 2). The length of the channels depends on the applied voltage, and the thickness is virtually constant and equal to ~100 micron [2].

The surface discharge has been experimentally and theoretically studied [5–7]. In the present paper, we report the results of a numerical study of a surface barrier discharge in oxygen at atmospheric pressure. Numerical modeling of the discharge was performed in the two-dimensional approximation assuming the existence of local equilibrium. The coordinate system is shown in Fig. 1.

The dynamics of charged and neutral particles in the discharge zone is described by the set of Boltzmann equations. Under the conditions of local equilibrium, the Boltzmann equations are transformed into the set of continuity equations:

$$\frac{\partial n_i}{\partial t} + \mathrm{div}(\bar{j}_i) = S_i, \quad (1)$$

$$\bar{j}_i = D_i \mathrm{grad}(n_i) + \bar{V}_i n_i, \quad (2)$$

where n_i, $\bar{j}_i$, D_i, S_i, and $\bar{V}_i$ are the density of charged particles, the current density, the diffusion coefficient, the source, and the velocity of the ith particle, respectively. For each charged particle, the source is thought of as integrals describing the processes of ionization, adhesion, and detachment of particles, as well as their dissociation. The mathematical model implies the presence of electrons and positive and negative ions. Two types of negative ions—atomic and molecular oxygen—are considered.

To solve the set of Eqs. (1) and (2), we determined the boundary and initial conditions. According to the discharge cell model, two types of surfaces exist: actual

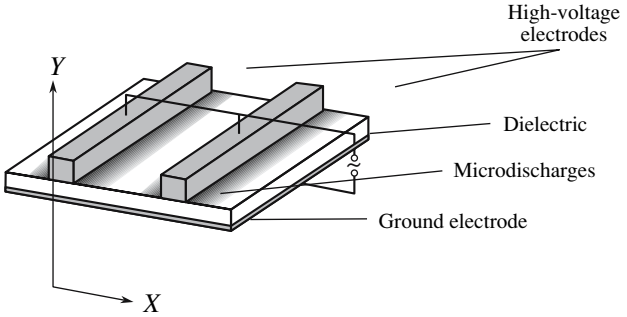

Fig. 1. Discharge cell of the surface barrier discharge.

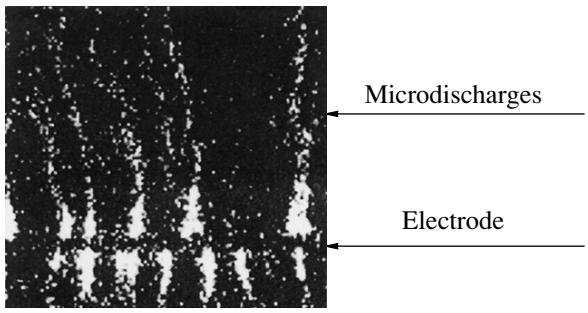

Fig. 2. Photograph of the surface layer of the barrier discharge [5].

(the surface of the electrode and dielectric) and virtual (the outer boundary of the discharge zone in a gas). The dielectric and electrode surfaces were considered as sources of secondary electrons that are due to photoemission and ion emission. The secondary electron density is related to the ion and photon flux to the surface by the equation

$$n_e V_e = \gamma_+ n_+ V_+ + \gamma_{ph}\phi, \quad (3)$$

where γ_+ is the secondary electron emission coefficient (these electrons appear when positive ions impinge the surface); γ_{ph} is the coefficient of electron photoemission from the cathode; V_+ and V_e are the magnitudes of the velocities of positive ions and electrons, respectively. The photon flux density ϕ at the cathode surface was taken to be proportional to the ionization rate in the discharge volume and was determined by integration over the entire discharge region. It was assumed that all particles arriving at the surface of the conducting high-voltage electrode are removed from the discharge region. All particles that arrive at the dielectric surface are deposited on it, and the charge of these particles was taken into account in calculation of the electric field strength. The particles that reached the outer boundaries of the discharge region can leave the integration region.

The initial conditions were as follows:

(1) The density of charged particles in the gas was taken to be zero.

(2) The initial charge density at the dielectric surface was determined by the preceding discharge.

To correct for the effect of cell diffusion in the calculation of the dynamics of charged particles, the FCT method was used [8]. To determine the electric field configuration in the discharge region, two integration regions were considered: the dielectric and the gas, which differ in permittivity. For each of the regions, the Poisson equation was solved:

$$\mathrm{div}(\bar{E}) = \frac{1}{\varepsilon_0 \varepsilon_i}\rho_i. \quad (4)$$

At the dielectric–gas interface, these solutions were combined by known relationships between the normal and tangential components of the electric field strength, taking into account the charge deposited onto the dielectric surface.

The distribution of potential at the open boundaries of the integration region was determined by integration of the charge distributions at the electrode and dielectric surfaces, as well as in the discharge region of the gas. The charge distribution at the electrode surface was determined taking into account that this surface should be equipotential [3].

Calculations were performed for the discharge in oxygen at atmospheric pressure. The dielectric had the relative dielectric constant 8.4 and the thickness 2 mm; the high-voltage electrode in cross section was a 3-mm square. The results below concern modeling of the dynamics of discharge processes of the surface barrier

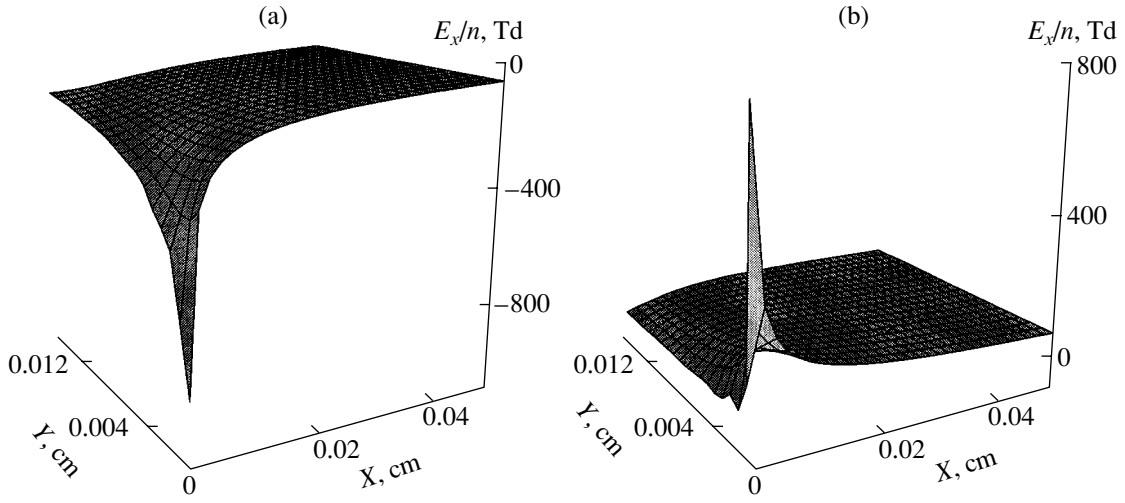

Fig. 3. Initial distribution of the electric field strength (a) along the dielectric surface and (b) normally to the dielectric surface.

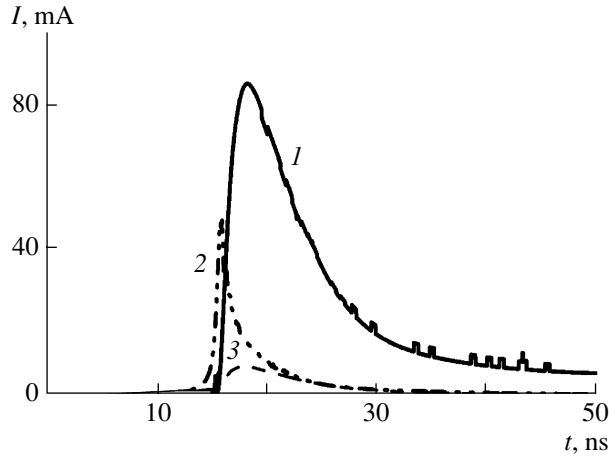

Fig. 4. (*1*) Total discharge current and (*2*, *3*) emission currents induced by (*2*) photoemission and (*3*) ion processes at the cathode surface.

discharge when a constant negative voltage is applied to the electrode.

Initial Stage of the Discharge and Formation of the Cathode Layer

The results of calculations of the field strength before the breakdown of the discharge gap are shown in Fig. 3. The gas breakdown conditions are met near the angle formed by the surfaces of the electrode and dielectric. In this region, with the characteristic size of several tens of microns, the appearance of electrons leads to the development of discharge processes.

The appearance of priming electrons in the discharge zone initiates the development of processes that eventually lead to the gas breakdown along the dielectric surface [4]. The total number of initial electrons does not exceed a few thousands. There is a definite delay between the instant of the appearance of initial electrons in the gas and the breakdown. Depending on the initial voltage on the electrode and the number of electrons, this delay amounts to a few nanoseconds. After the delay, the current discharge pulse is observed (Fig. 4). The same figure also shows the plots of emission currents induced by photoemission and ion emission processes at the cathode surface. As is seen, the appearance of the major discharge current is preceded by a considerable photocurrent. The discharge current front lasts for a few nanoseconds, whereas the complete duration of the discharge current is as long as 20–25 ns.

Photoemission is of crucial importance for initiation of discharge processes. The exclusion of photoemission processes from the model leads to a considerable (by one order of magnitude or more) delay of the front of the discharge current, to an equal increase in its complete duration, and a decrease in its amplitude, which is inconsistent with experimental data [5, 6]. As the discharge current builds up, the role of photo processes decreases; at the same time, a noticeable emission current appears, which is caused by collisions of positive ions with the cathode surface.

The change in the significance of emission processes, as well as the buildup of the discharge current, is associated with rearrangement of the electric field configuration near the cathode (Fig. 5). First of all, the field strength near the cathode increases by about 30% and becomes as large as 1500 Td, which follows from comparison of Figs. 3 and 5. In addition, the longitudinal component of the electric field strength approaches closely the cathode. Simultaneously with this process, the region with high field strength along the cathode surface expands from the dielectric surface to the upper edge of the cathode (Fig. 6). The parameters of the cathode layer of the surface barrier discharge are virtually the same as the parameters of the ordinary cathode layer of the glow discharge; i.e., in a few nanoseconds, an ordinary cathode layer is formed at the cathode surface. The change in its transverse sizes along the cath-

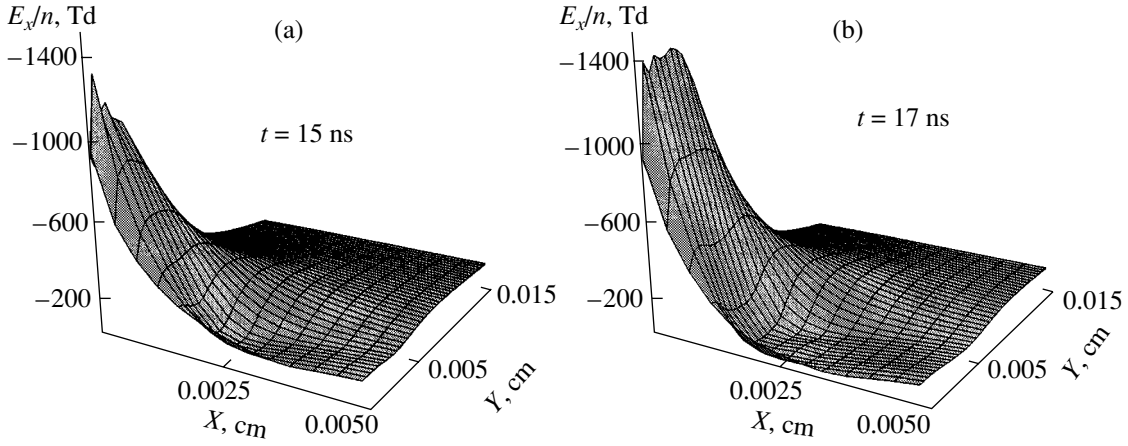

Fig. 5. Formation of the cathode layer at t = (a) 15 and (b) 17 ns.

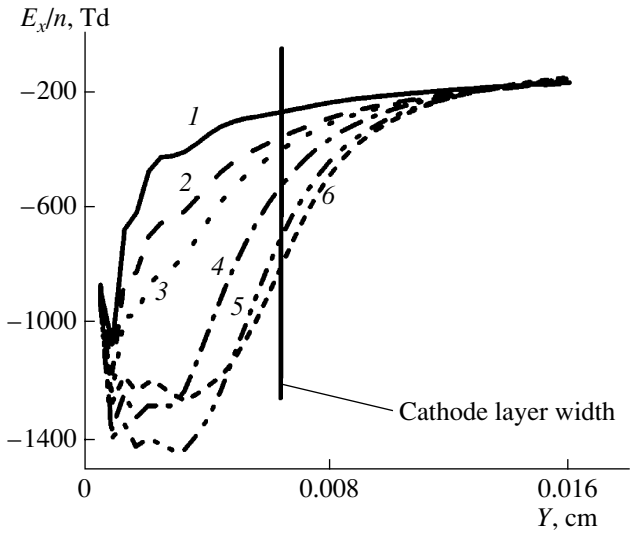

Fig. 6. Expansion of the cathode spot at the cathode surface at t = (*1*) 1, (*2*) 15.2, (*3*) 15.5, (*4*) 16, (*5*) 17, and (*6*) 18.8 ns.

ode surface is the process known as cathode spot expansion.

The expansion takes place simultaneously with the development of the discharge current front. Near the current maximum, the transverse size of the cathode spot is stabilized: its size is as large as 40–60 micron (Fig. 6). The longitudinal thickness of the cathode layer is about 20–30 micron. The current density at the outer boundary of the cathode layer is as large as 250 A/cm^2. All these parameters are virtually coincident with the parameters of the ordinary cathode layer in oxygen at atmospheric pressure.

CONCLUSIONS

Thus, the numerical modeling of the processes in the surface barrier discharge showed that

(1) the breakdown begins with a sharp enhancement of photoemission from the cathode surface;

(2) the increase in the secondary emission from the electrode surface leads to the formation of the cathode layer, and the cathode spot at the surface of the conducting electrode expands until the charge deposited onto the dielectric surface stops this process;

(3) in the developed cathode layer, the role of photo processes in the discharge dynamics decreases and is replaced by the secondary electron emission induced by impingement of positive ions onto the cathode surface.

REFERENCES

1. Lunin, V.V., Popovich, M.P., and Tkachenko, S.N., *Fizicheskaya khimiya ozona* (Physical Chemistry of Ozone), Moscow, 1998, p. 480.
2. Kogelschatz, U., *IEEE Trans. Plasma Sci.*, 2002, vol. 30, p. 1400.
3. Gibalov, V.I. and Pietsch, G.J., *J. Phys. D: Appl. Phys.*, 2000, vol. 33, p. 2618.
4. Gibalov, V.I. and Pietsch, G.J., *J. Phys. D: Appl. Phys.*, 2004, vol. 37, p. 2093.
5. Saveliev, A.B., Gibalov, V.I., and Pietsch, G.J., *Proc. 14 ISPC*, Prague, 1998, p. 2343.
6. Kozlov, M.V. Sokolova, M.V., et al., *Plasmas Polym.*, 2003, vol. 8, p. 179.
7. Humpert, C. and Pietsch, G.J., *Ozone: Sci. Eng.*, 2005, vol. 27, p. 59.
8. Book, D.L., Boris, J.P., and Hain, K.J., *Comput. Phys.*, 1975, vol. 20, p. 248.